

## NUCLEAR ISOMERS $^{90m,g}\text{Zr}$ , $^{89m,g}\text{Zr}$ , $^{89m,g}\text{Y}$ AND $^{85m,g}\text{Sr}$ FORMED BY BOMBARDMENT OF $^{89}\text{Y}$ WITH PROTONS OF ENERGIES FROM 4 TO 40 MeV

B. SATHEESH\* and M. M. MUSTHAFA†

*Department of Physics, University of Calicut,  
Calicut University P.O. Malappuram, Kerala 673635, India*

\*satheesh.b4@gmail.com

†mm\_musthafa@rediffmail.com

B. P. SINGH and R. PRASAD

*Department of Physics, Aligarh Muslim University,  
Aligarh, Uttar Pradesh 202002, India*

Accepted 1 June 2011

Excitation functions for the reactions  $^{89}\text{Y}(p,n)^{89g}\text{Zr}$  and  $^{89}\text{Y}(p,n)^{89m}\text{Zr}$  have been measured over the energy ranges from threshold to 15 MeV using stacked foil activation technique. The isomeric cross-section ratio  $\sigma_m/(\sigma_m + \sigma_g)$  for the formation of  $^{89m,g}\text{Zr}$  was determined. The excitation functions and isomeric cross-section ratios were calculated for the reactions  $^{89}\text{Y}(p,\gamma)^{90m,g}\text{Zr}$ ,  $^{89}\text{Y}(p,n)^{89m,g}\text{Zr}$ ,  $^{89}\text{Y}(p,p)^{89m,g}\text{Y}$  and  $^{89}\text{Y}(p,\alpha n)^{85m,g}\text{Sr}$  also for energy range 4–40 MeV. The PE emission fraction is found to depend strongly on the energy of the incident particle. The isomeric cross-section ratio is found to depend strongly on the relative spins of the isomeric and ground state and some dependence on energy difference between the levels.

*Keywords:* Excitation functions; stacked foil activation technique; PE emission; isomeric cross-section ratio.

PACS Number(s): 24.60.Dr, 25.60.Gr, 24.40.-h

### 1. Introduction

The nuclear reaction mechanism is usually considered to be the tool to study the properties of the nucleus and the nature of nuclear force. Pre-Equilibrium (PE) emission process has been identified as the prominent reaction mechanism at intermediate energies. The signatures of PE emission can often be observed in the excitation functions, angular distribution and energy spectra of emitted particles.<sup>1</sup> A few nuclei are taking part in interaction mechanism causing the emission of particles with relatively higher energies. Opening of successive channels will be suppressed leading to the slowly descending tails of excitation functions. Dependence of the relative contribution of PE emission on incident energy and angular momentum

provide information on the relative progress of the reaction mechanism and the equilibration mechanism of the compound nucleus.<sup>2-7</sup> The study of the formation of nuclear isomeric pairs in nuclear reactions will provide important information on the angular momentum transfer, gamma de-excitation processes and coupling of channels during the reaction processes.<sup>8-12</sup> This is very important in the case of highly deformed nucleus, where states with larger value of projection quantum number  $K$  are produced.<sup>13</sup> Qaim *et al.* have shown<sup>14</sup> that the isomeric cross-section ratio is primarily governed by the spins of the two levels involved, rather than their separation and excitation energies. However it is quite possible that the onset of PE emission at relatively higher incident energies may distort this smooth behavior. Keeping the above facts in mind, as a part of systematic study of nuclear reactions induced by light and heavy ions, we determined the excitation functions for the reactions  $^{89}\text{Y}(p, \gamma)^{90m,g}\text{Zr}$ ,  $^{89}\text{Y}(p, n)^{89m,g}\text{Zr}$ ,  $^{89}\text{Y}(p, p)^{89m,g}\text{Y}$  and  $^{89}\text{Y}(p, \alpha n)^{85m,g}\text{Sr}$  and the isomeric population ratios for the production of isomeric pairs of  $^{90m,g}\text{Zr}$ ,  $^{89m,g}\text{Zr}$ ,  $^{89m,g}\text{Y}$  and  $^{85m,g}\text{Sr}$  nuclei formed in the above reactions for energy ranges from threshold to 40 MeV.  $^{89}\text{Y}$  is an important material widely applied to increase the strength of alloys of important metals of nuclear technology (aluminum, magnesium and chromium). The proton induced activation cross-section of this element is important for dose estimation in accelerator technology, for thin layer activation (TLA) analysis of yttrium alloys and yttrium oxide ceramics.<sup>15,16</sup> Yttrium is a mono isotopic element and therefore is an ideal target material to test nuclear reaction theories. Experimentally measured cross-sections for the reactions  $^{89}\text{Y}(p, n)^{89m,g}\text{Zr}$  over the energy range  $\sim 5-15$  MeV, have been used as the standard reference for evaluating cross-sections for other cases. Theoretical estimation of the cross-sections for the above reactions have been done using the nuclear reaction code EMPIRE-II.<sup>17</sup> Isomeric cross-section ratio is calculated as the ratio of production of isomeric state to the total production of the particular nucleus at the given incident energy.

## 2. Experiment and Analysis

Experiment has been performed at the variable energy cyclotron center (VECC), Kolkata, India, employing stacked foil activation technique. The Yttrium samples of thickness  $\sim 3.32$  mg/cm<sup>2</sup>, were prepared by centrifugal method of Y<sub>2</sub>O<sub>3</sub> on Aluminum backing. A stack of nine such samples were irradiated using diffused beam of proton of energy 15 MeV with a beam current of 100 nA for 12 hrs. Suitable thickness of Aluminum degraders were introduced between the samples to have desired energy falling on each sample in the stack. The energy degradation in the sample thickness, backing and degraders are taken into account. The average beam energy on each target was calculated using stopping power values for Yttrium and Aluminum at various energies taken from Nuclear Data Tables.<sup>18</sup> The beam flux was monitored continuously through current integrator connected to the Faraday cup kept behind the target stack. The activities induced in each sample were followed using a 100 cc HPGe detector coupled to the ORTEC's PC based multichannel

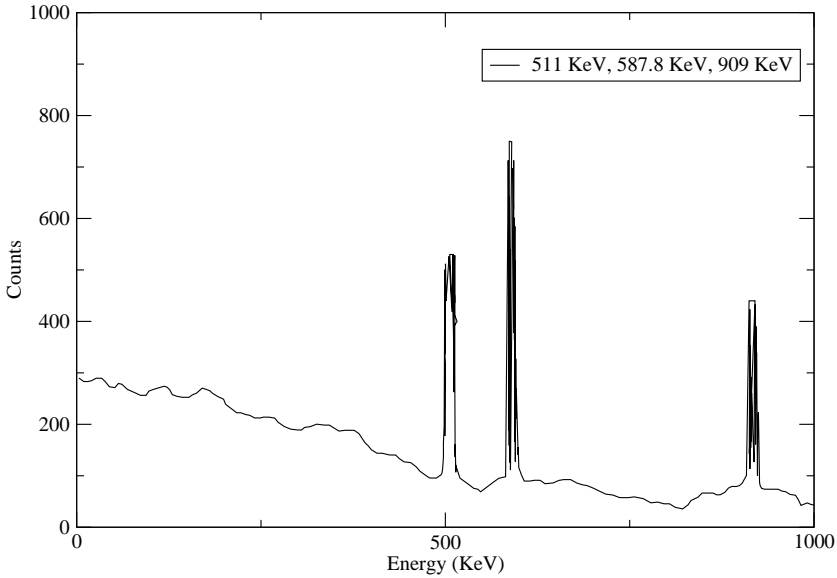


Fig. 1. Observed gamma ray spectrum from  $^{89}\text{Y}$  irradiated with 15 MeV proton.

analyzer at the Inter University Consortium for DAE facilities, Kolkata Center. In order to follow the activity of the short life time of 4.16 min for isomeric state of  $^{89}\text{Zr}$  the activity was measured within 5 min of stopping of the irradiation in a separate run of short duration of 30 min. The geometry dependent efficiency of the detector for various gamma energies at different source-detector distances were determined using standardized  $^{152}\text{Eu}$  point source, which was also used for the calibration of detector system. From the measured activity of each nucleus in the sample the reaction cross-section at given energy is calculated using the formula given elsewhere.<sup>19</sup> A typical gamma ray spectra of the  $^{89}\text{Y}$  sample irradiated with 15 MeV proton beam is given in Fig. 1. Since short activity and the longer activity were induced in separate runs and measured separately, the spectra shown in Fig. 1 is the superposed spectra of two measurements.

In this way, the excitation functions for the reactions  $^{89}\text{Y}(p, n)^{89g}\text{Zr}$  and  $^{89}\text{Y}(p, n)^{89m}\text{Zr}$  were measured separately and are plotted in Fig. 2. The error indicated by the error bar in this measured data are the sum of all the possible errors involved in the measurement. This may be due to the following factors (a) statistical uncertainty in the Gamma counting, (b) uncertainty in determining the number of target nuclei in the sample due to non uniform deposition of the target material, (c) fluctuation in the beam current, (d) inaccuracy in the determination of geometry dependent detector efficiency of the Gamma spectrometer, (e) beam intensity loss as the beam traverses the thickness of the target stack materials, (f) product nuclei recoiling out of the sample target foil and, (g) dead time loss etc. A detailed error analysis of the similar measurement is given in Ref. 19. However the maximum

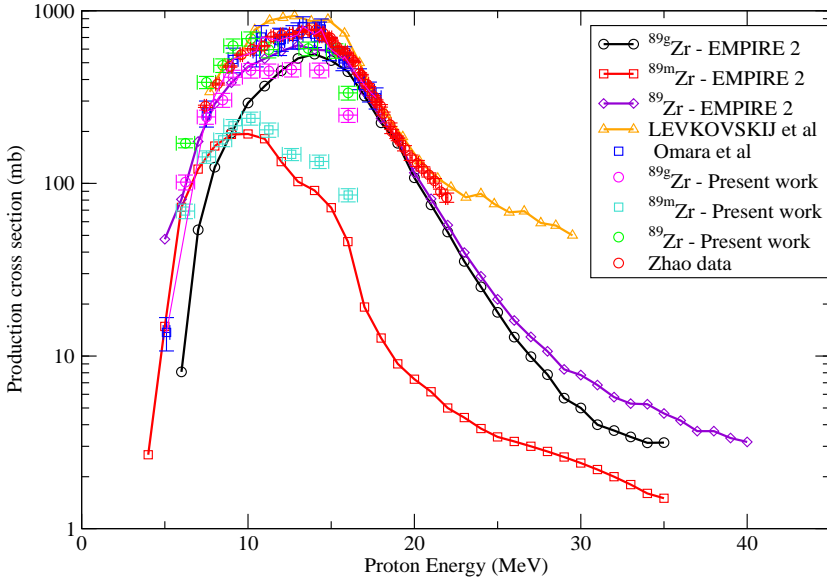


Fig. 2. (Color online) Experimentally measured and theoretically calculated excitation functions for the reaction  $^{89}\text{Y}(p, n)^{89}\text{Zr}$ . Experimental data from Refs. 20–22 are also shown in the figure.

error accumulated due to all the above factors is estimated to be less than 13%. In order to make a comparative study of the measured data the literature data for the same reaction measured by Levkovskij,<sup>20</sup> Zhao *et al.*<sup>21</sup> and, Omara *et al.*<sup>22</sup> are also plotted in Fig. 2. To the best of our knowledge no experimental data for separate ground state and isomeric cross-section data are available in literature. Hence the literature data are compared with the excitation functions for total reaction cross-sections (sum of ground state and isomeric state). The literature data are in satisfactory agreement with the present measurement, except that of Levkovskij which is slightly higher in the peak region. No straight forward explanation could be given for this discrepancy. However, it is to be noted that there is no estimation of error given in this data.

### 3. Theoretical Analysis

Theoretical analysis of the data has been performed using the nuclear reaction code EMPIRE-II. This code makes use of the Hauser–Feshbach model<sup>23</sup> for the statistical part of the nuclear reaction which treats nuclear reaction through compound nucleus formation and subsequent decay of the compound nucleus. The NVWY model<sup>24</sup> based on MSD–MSC (Multi Step Direct–Multi Step Compound) approach<sup>25</sup> and the exciton model<sup>26</sup> are used for the PE emission part. The Hauser–Feshbach model explicitly takes into account the conservation of spin and parity of each partial wave in each stage of de-excitation. This approach helps in evaluating the population of isomeric state and hence the determination of isomeric cross-section ratio which is

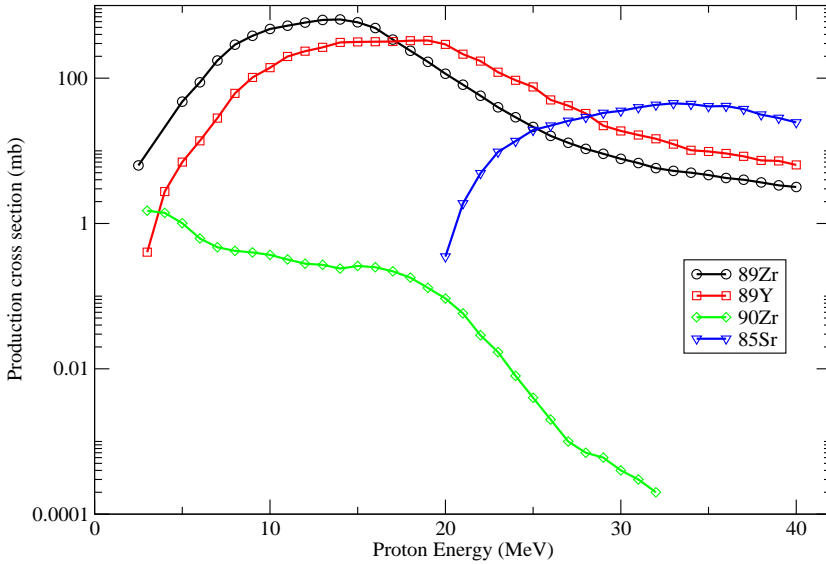


Fig. 3. (Color online) Theoretically calculated excitation functions for the reactions  $^{89}\text{Y}(p, n)^{89}\text{Zr}$ ,  $^{89}\text{Y}(p, p)^{89}\text{Y}$ ,  $^{89}\text{Y}(p, \gamma)^{90}\text{Zr}$ ,  $^{89}\text{Y}(p, \alpha n)^{85}\text{Sr}$  using EMPIRE-II. Calculations are performed at 1 MeV steps.

of much interest in the present work. For input parameters standard library<sup>27</sup> is used; which include the nuclear masses, ground state deformations, discrete levels and level schemes, moment of inertia and gamma ray strength functions. The particle transmission coefficients for both the exciton and Hauser–Feshbach formalism were generated via the spherical optical model. Optical model parameters due to Koning<sup>28,29</sup> have been used in the present calculation for both protons and neutrons. The nuclear masses are taken consistently from Table of Isotopes<sup>30</sup> and the energy levels and decay schemes are taken from Table of Radioactive Isotopes.<sup>31</sup> Effects of the dynamic deformations of fast rotating nucleus are taken into account in the calculations. Initial exciton number is an important parameter in PE emission calculation, the value of which is consistently taken as 3 ( $= 2p + 1h$ ), which may be interpreted as the projectile on interaction with the target nucleus excites one particle above the Fermi level leaving a hole in the Fermi level. The transition matrix element for the intranuclear transition is taken from Serber.<sup>32</sup> The cross-sections for the production of each nucleus (for isomeric and ground population separately) are determined. The excitation functions, thus calculated for the reactions  $^{89}\text{Y}(p, n)^{89g}\text{Zr}$ ,  $^{89}\text{Y}(p, n)^{89m}\text{Zr}$  are also shown in Fig. 2, along with the experimental data separately for ground state, isomeric state and the total production. The parametrization in the code as above reproduce satisfactorily well over the measured energy range. In order to estimate the production of other isotopes of interest such as  $^{90}\text{Zr}$ ,  $^{89}\text{Zr}$ ,  $^{89}\text{Y}$  and  $^{85}\text{Sr}$  produced in the present case, the excitation functions for the reactions  $^{89}\text{Y}(p, \gamma)^{90}\text{Zr}$ ,  $^{89}\text{Y}(p, n)^{89}\text{Zr}$ ,  $^{89}\text{Y}(p, p)^{89}\text{Y}$  and

$^{89}\text{Y}(p, \alpha n)^{85}\text{Sr}$  were also calculated using the code EMPIRE-II with same parameter sets as mentioned above and are shown in Fig. 3.

### 4. Result and Discussion

In the above figures the high energy portions of the excitation functions give clear indication of PE emission. In order to estimate the relative contribution of PE emission at each energies calculation was performed with and without including PE part of the calculation and are shown in Fig. 4. It can be seen from Fig. 4 that in the present case, the excitation functions for  $^{89}\text{Y}(p, n)^{89}\text{Zr}$  reaction shows significant amount of PE emission where as the excitation function for the  $^{89}\text{Y}(p, p)^{89}\text{Y}$  reaction is unchanged on including and excluding the PE emission. Thus it is assumed that the PE emission prefer neutron emission over the proton emission and the proton emission is to be taking place after equilibration of the compound nucleus. Similarly alpha emission in the  $\alpha n$  channel is also expected to be taking place

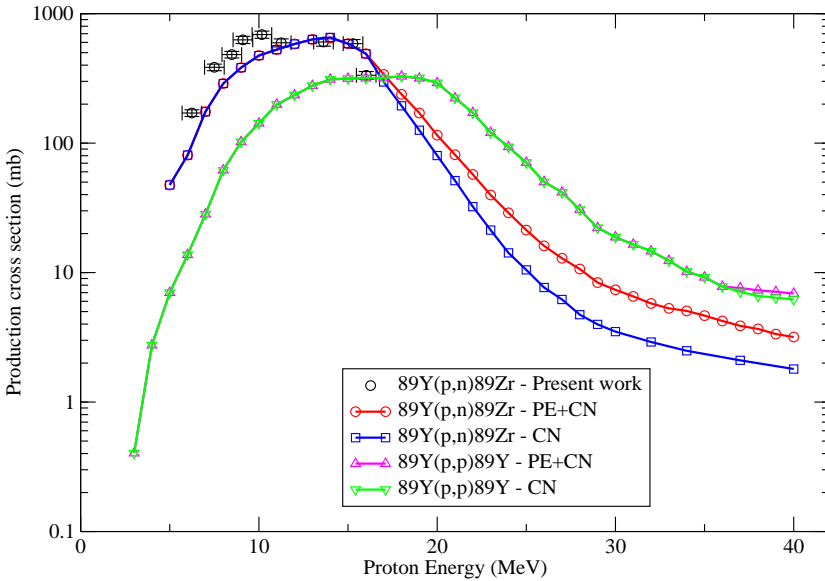


Fig. 4. (Color online) Experimentally measured and theoretically calculated excitation functions for the reactions  $^{89}\text{Y}(p, n)^{89}\text{Zr}$ ,  $^{89}\text{Y}(p, p)^{89}\text{Y}$ .

Table 1. Spins of the relevant states of the isomeric nuclides of interest.

Nuclide	Ground state			Meta stable state		
	Energy (MeV)	Spin and parity	$T(1/2)$	Energy (MeV)	Spin and parity	$T(1/2)$
$^{90}\text{Zr}$	0	$0^+$	stable	2.3187	$5^-$	809.2 ms
$^{89}\text{Zr}$	0	$9/2^+$	78.41h	0.5878	$1/2^-$	4.16 m
$^{89}\text{Y}$	0	$1/2^-$	stable	0.909	$9/2^+$	16.1 s
$^{85}\text{Sr}$	0	$9/2^+$	64.84d	0.2387	$1/2^-$	67.63 m

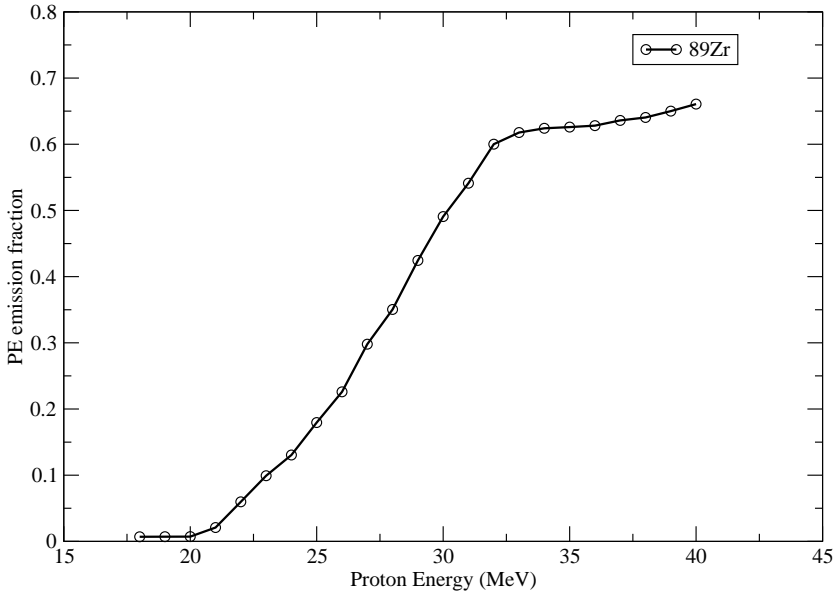


Fig. 5. Variation of PE emission fraction as a function of incident energy.

after the equilibration. The relative strength of the PE emission is expressed as the PE fraction of PE emission contribution to the total production cross-section  $(\sigma_{ER} - \sigma_{CN})/\sigma_{ER}$ , where  $\sigma_{ER}$  is the cross-section for the production of given evaporation residue including equilibrium and PE emission contributions and  $\sigma_{CN}$  is the cross-section calculated as statistical equilibration of the compound nucleus without PE emission. The PE emission fraction thus determined for the reaction is plotted in Fig. 5.

The PE emission contribution starts significantly for incident energy above 18 MeV. This is also evident from the observed sudden fall of excitation functions for reaction  $^{89}\text{Y}(p, \gamma)^{90}\text{Zr}$  reaction at about 18 MeV, where the PE emission mechanism prevents the statistical formation of equilibrated compound nucleus  $^{90}\text{Zr}$  at higher energies. The PE emission contribution increases sharply with incident energy over the energy range 19–33 MeV and get saturated thereafter. Most of the previous works on proton induced reactions indicate<sup>33,34</sup> that PE emission contribution increases steadily with the incident energy at about 12 MeV. Small values of PE emission fraction for energies from 12 to 19 MeV and sharp increases from energies 19 MeV in the present case may be attributed to the shell closure of the nucleus at  $N = 50$  and  $Z = 40$  which may hinder the PE emission up to certain excitation energies (19 MeV in the present case). Similar trend of hindering PE emission is also seen in the case of  $^{51}\text{V}$ ,<sup>35</sup> where neutron shell closure occurs at  $N = 28$ . Similarly the enhanced cross-section for  $4n$  channel compared to  $3n$  and  $5n$  channels in the case of  $^{198}\text{Pt}(^{20}\text{F}, 4n)^{213}\text{Fr}$  reaction<sup>36</sup> and observed fission frag-

ment anisotropies for  $^{12}\text{C} + ^{194,198}\text{Pt}$  systems<sup>37</sup> are attributed to the shell closure at  $N = 126$ .

#### 4.1. Isomeric cross-section ratio in various reaction channels

The isomeric cross-section ratio is defined as the ratio of the formation cross-section of the isomer of high isomeric state to the total production cross-section  $\sigma_m/(\sigma_m + \sigma_g)$ . In the present case a number of isotopes having isomeric states of measurable half lives of the order of few minutes to few days are produced. In order to observe the relative population of ground state and isomeric state at various incident energies and the effect of various factors like relative spins, level difference and incident energy, the isomeric cross-section ratio for the production of  $^{89}\text{Zr}$  over the energy ranges from threshold up to 15 MeV for the reaction  $^{89}\text{Y}(p, n)^{89}\text{Zr}$  was determined from the measured cross-sections for the isomeric state and ground state at each energy and is plotted in Fig. 6, along with the theoretically calculated values up to the projectile energy of 40 MeV. The calculated values of isomeric cross-section ratio for  $^{89}\text{Zr}$  agree well with the experimental data over the measured energy range. Similarly, the isomeric cross-section ratios for the production of  $^{90}\text{Zr}$ ,  $^{89}\text{Y}$  and  $^{85}\text{Sr}$  in the reactions  $^{89}\text{Y}(p, \gamma)^{90}\text{Zr}$ ,  $^{89}\text{Y}(p, p)^{89}\text{Y}$  and  $^{89}\text{Y}(p, \alpha n)^{85}\text{Sr}$  respectively are determined as above and are also plotted in Fig. 6. For the sake of completeness the excitation functions for the ground state populations and isomeric

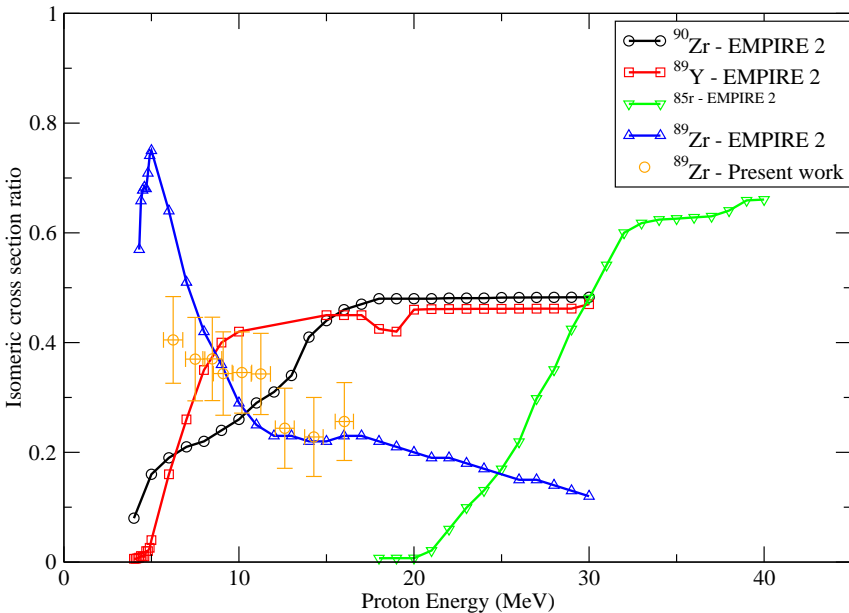


Fig. 6. (Color online) Isomeric cross-section ratio  $\sigma_m/(\sigma_m + \sigma_g)$ , for the isomeric pairs  $^{90}\text{Zr}$ ,  $^{89}\text{Zr}$ ,  $^{89}\text{Y}$  and  $^{85}\text{Sr}$  in the reactions  $^{89}\text{Y}(p, \gamma)^{90}\text{Zr}$ ,  $^{89}\text{Y}(p, n)^{89}\text{Zr}$ ,  $^{89}\text{Y}(p, p)^{89}\text{Y}$ , and  $^{89}\text{Y}(p, \alpha n)^{85}\text{Sr}$  respectively.

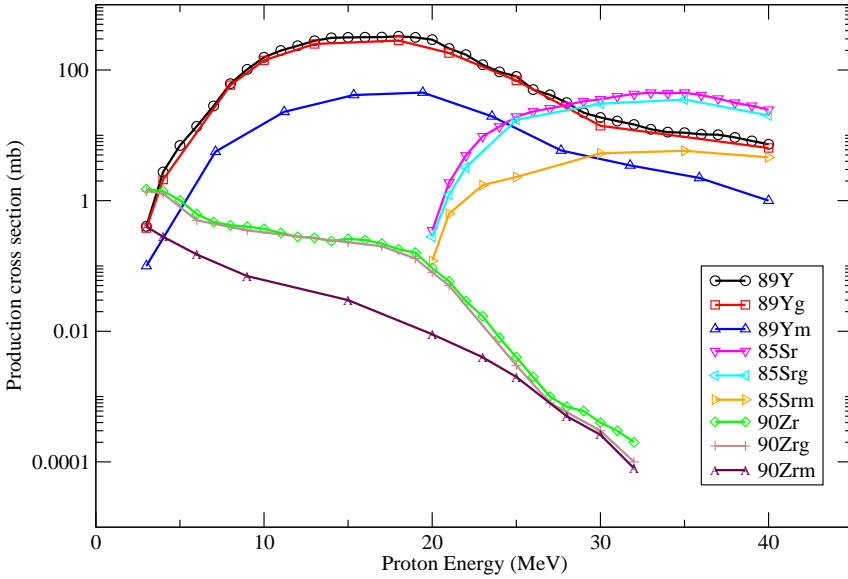


Fig. 7. (Color online) Theoretically calculated excitation functions for ground state, isomer state and the total for the reactions  $^{89}\text{Y}(p,p)^{89}\text{Y}$ ,  $^{89}\text{Y}(p,\alpha n)^{85}\text{Sr}$ ,  $^{89}\text{Y}(p,\gamma)^{90}\text{Zr}$ .

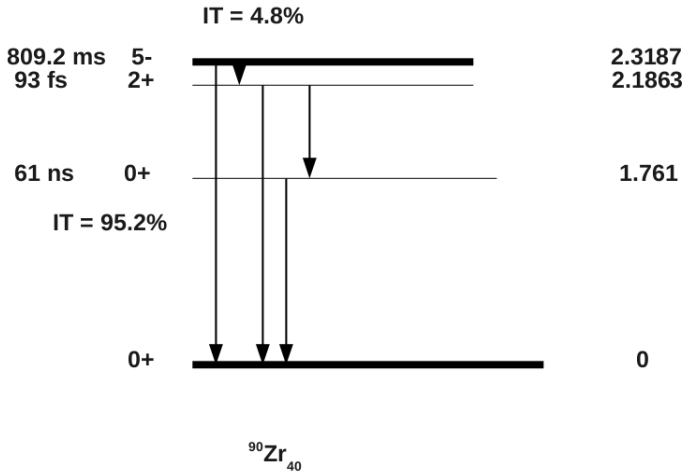


Fig. 8. Decay scheme of  $^{90}\text{Zr}$ . The energy levels in terms of MeV.

state populations for this nuclei are separately plotted and are shown in Fig. 7. The relevant parameters like spin, energies and life time of the ground and excited states for the nuclei of interest are summarized in Table 1 and associated decay schemes are given in Figs. 8–10.

Both theoretical calculations and experimental analysis indicate that the isomeric cross-section ratio has reflection on the relative level difference between the

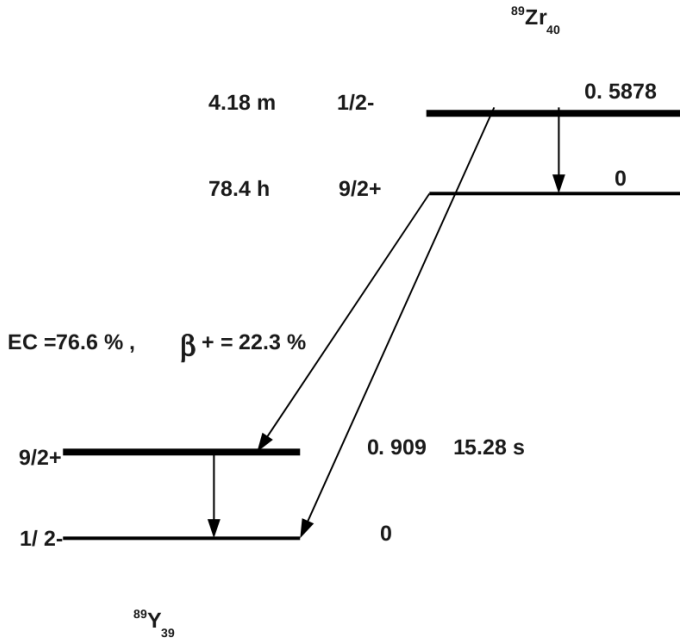


Fig. 9. Decay scheme of  $^{89}\text{Zr}$ . The energy levels in terms of MeV.

isomeric state and ground state as well as the spin of the states. At relatively larger energies the system seems to prefer higher spin states rather than the excitation energy available for the system as is indicated by relative population of the above nuclei. In the case of  $^{89}\text{Zr}$  nucleus the isomeric cross-section ratio is found to be increasing sharply with incident energy up to a value of 0.78 at 5 MeV, falls steadily to a value of 0.2 at about 12 MeV and thereafter it remains almost fixed at this value for higher incident energies. In the case of  $^{89}\text{Y}$  nucleus, for the 5–10 MeV incident proton energy range, the isometric cross-section ratio increases steadily and reaches a stable value of 0.5 for energies above 10 MeV. In the case of  $^{90}\text{Zr}$ , the ratio increases steadily to a value of 0.2 for the range up to 6 MeV and shows very small increments up to 12 MeV. Above 12 MeV, the ratio raises steadily and reaches a saturation value of 0.5 at 15 MeV. The  $^{85m,g}\text{Sr}$  is expected to follow the nature of  $^{89}\text{Zr}$ . The  $^{85m,g}\text{Sr}$  is expected to follow the nature of  $^{89}\text{Zr}$ . This nature of isomeric cross-section ratio can be interpreted in terms of relative spins and energy levels. In the case of  $^{89}\text{Zr}$ , the ground state spin is  $9/2^+$  and isomeric state spin is  $1/2^-$  at energy of 0.5878 MeV. Thus at lower energies only the ground state is populated irrespective of spin state. As the energy increases higher state starts getting populated and on further increase of energy, larger angular momentum is transferred to the nucleus with preferable population of  $9/2^+$  state. In the case of  $^{89}\text{Y}$  the ground state spin is  $1/2^-$  and isomeric state spin is  $9/2^+$  at energy of 0.909 MeV. The population starts with the ground state and the isomer state with

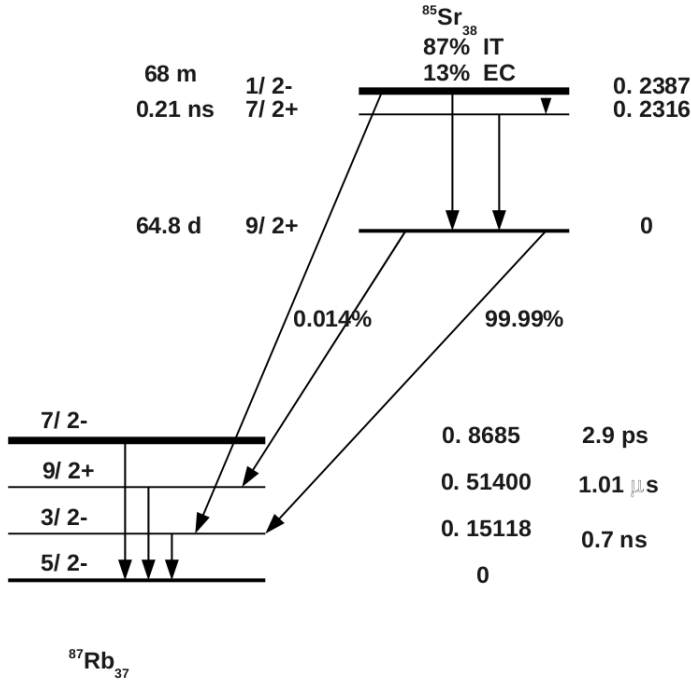


Fig. 10. Decay scheme of  $^{85}\text{Sr}$ . The energy levels in terms of MeV.

higher spin of  $9/2^+$ . As the high energy state prefer higher spin state, the isomeric cross-section ratio increases sharply in the beginning and easily get saturated. Similarly in the case of  $^{90}\text{Zr}$  the ground state spin is  $0^+$  and isomeric state spin is  $5^-$  at energy of 2.3187 MeV with intermediate state of  $0^+$  at 1.761 MeV and  $2^+$  at 2.1863 MeV. Thus the isomeric state of higher spin  $5^-$  is gradually populated after populating intermediate states of  $0^+$  and  $2^+$  and get saturated at higher angular momentum state. The  $^{85}\text{Sr}$  follows exactly the similar nature with ground state spin of  $9/2^+$  and isomeric state of  $1/2^-$  at 0.2387 MeV and an intermediate state of  $7/2^+$  at 0.2316 MeV. Thus the angular momentum transfer and population of higher levels in the production of any nuclei depends upon the relative spins and energy levels. Lesser the energy difference sharper will be the change in the ratio, where as the presence of intermediate states causes slower rate of change of the relative population between the states. Further, in the Fig. 7, sudden change in the isomeric cross-section ratio at energies between 18–21 MeV in the case of  $(p, n)$  and  $(p, p)$  reactions may be attributed to the PE emission. This may be justified as the PE emission in the present case starts significantly at about 19 MeV where the out going particle (proton or neutron) carries larger angular momentum leaving the residual nucleus in relatively lower angular momentum state and hence higher population of isomeric state with lower spin. The system comes to saturation value again thereafter.

## 5. Conclusion

The PE emission probability increases with increasing incident energy. The onset of PE emission is affected critically by the neutron shell closure. The isomeric cross-section ratio strongly depends on relative spins, energy difference and the presence of intermediate states between the ground and the isomeric states and the spin states of such intermediate states as well as on the onset of PE emission. The PE emission particles carry larger angular momentum.

## Acknowledgments

The authors thank the VECC personnel for all their help and cooperation during the experiments. Authors are also thankful to the Head of the Department, Department of Physics, Calicut University, Kerala, India, for providing necessary facilities to carry out this work. One of the author (B. Satheesh) acknowledges the financial support from Kerala Government in the form of fellowship.

## References

1. H. Ejiri et al., *Nucl. Phys. A* **305** (1978) 167.
2. M. Blann, *Annu. Rev. Nucl. Sci.* **25** (1975) 123.
3. J. Pal, C. C. Dey, P. Banerjee, S. Bose, B. K. Sinha and M. B. Chatterjee, *Phys. Rev. C* **71** (2005) 03605.
4. S. Mukherjee, N. L. Singh, G. K. Kumar and L. Chaturvedi, *Phys. Rev. C* **72** (2005) 014609.
5. E. Gadioli, E. Gadioli-Ebra, J. J. Hogan and B. V. Jacab, *Phys. Rev. C* **29** (1984) 76.
6. M. K. Sharma, H. D. Bhardwaj, Unnati, P. P. Singh, B. P. Singh and R. Prasad, *Eur. Phys. J. A* **31** (2007) 43.
7. A. Kaplan, A. Ayain, E. Tel and B. S. Arer, *Pramana* **72**(2) (2009) 343.
8. C. L. Rao and L. Yaffe, *Can. J. Chem.* **50** (1972) 1877.
9. D. R. Sachdev and L. Yaffe, *Can. J. Chem.* **45** (1967) 2711.
10. D. R. Sachdev and L. Yaffe, *Can. J. Chem.* **47** (1969) 1667.
11. J. H. Forster and L. Yaffe, *Can. J. Chem.* **46** (1968) 1763.
12. A. H. Khan, G. B. Saha and L. Yaffe, *Can. J. Chem.* **47** (1969) 3817.
13. H. Ejiri et al., *Phys. Lett. B*, **78**(2) (1978) 3.
14. S. M. Qaim, S. Sudar and A. Fessler, *J. Radiochim. Acta* **93** (2005) 503.
15. M. S. Uddin and M. Baba et al., *J. Nucl. Sci. Tech.* **160** (2004).
16. M. S. Uddin, M. Hagiwara, F. Tarkanyi, F. Ditroi and M. Baba, *Appl. Radiat. Isotopes* **60** (2004) 911.
17. M. Hermann et al., *EMPIRE-II, Nuclear Reaction Model Code 2.19*, Nuclear Data Section (IAEA, Vienna, 2005).
18. L. C. Northcliffe and R. F. Schilling, *Nucl. Data Tables A* **7** (1970) 256.
19. M. M. Musthafa, B. P. Singh, M. G. V. Sankaracharyulu, H. D. Bhardwaj and R. Prasad, *Phys. Rev. C* **52** (1995) 6.
20. V. N. Levkovskij, *Activation Cross-Section by Protons and Alphas* (Moscow, USSR, 1991).
21. Z. Wenrong, S. Qingbiao, Luhalin and Y. Weixiang, *Chin. J. Nucl. Phys.* **14** (1992).

22. H. M. Omara, K. F. Hassan, S. A. Kandil, F. E. Hegazy and Z. A. Saleh, *Radiochim. Acta* **97** (2009) 467.
23. W. Hauser and H. Feshbach, *Phys. Rev.* **87** (1952) 366.
24. H. Nishioka, J. J. M. Verbaarschot, H. A. Wiedenmuller and S. Yoshida, *Ann. Phys.* **172** (1986) 67.
25. T. Tamura, T. Udagawa and H. Lenseke, *Phys. Rev. C* **26** (1982) 379.
26. E. Betak and P. Oblozinsky, Report INDC (SLK-001), IAEA Vienna (1993).
27. P. Moller and J. R. Nix, *Atom. Data Nucl. Data Tables* **26** (1981) 165.
28. A. J. Koning and J. P. Delaroche, *Nucl. Phys. A* **713** (2003) 213.
29. A. J. Koning and J. M. Akkermans, *Phys. Rev. C* **47** (1993) 724.
30. C. M. Lederer and V. S. Shirley, *Table of Isotopes* (Wiley, New York, 1978).
31. E. Brown and R. B. Firestone, *Table of Radioactive Isotopes* (Wiley, New York, 1986).
32. R. Serber, *Phys. Rev.* **72** (1947) 1114.
33. B. P. Singh, M. K. Sharma, M. M. Musthafa, H. D. Bhardwaj and R. Prasad, *Nucl. Instrum. Methods Phys. Res. Sect. A* **562** (2006) 717.
34. M. M. Musthafa, Ph.D. thesis, AMU, Aligarh, India (1996).
35. M. M. Musthafa, M. K. Sharma, B. P. Singh and R. Prasad, *Appl. Radia. Isotopes* **62** (2005) 419.
36. K. Mahata, S. Kailas, A. Shrivastava, A. Chatterjee, P. Singh, S. Santra and B. S. Tomar, *Phys. Rev. C* **65** (2002) 034613.
37. A. Shrivastava, S. Kailas, A. Chatterjee, A. M. Samant, A. Navin, P. Singh and B. S. Tomar, *Phys. Rev. Lett.* **82** (1999) 4.